

The Repressor-Lattice: Feedback, Commensurability, and Dynamical Frustration.

Mogens H. Jensen, Sandeep Krishna and Simone Pigolotti*
Niels Bohr Institute, Blegdamsvej 17, DK-2100, Copenhagen, Denmark[†]
(Dated: October 2, 2018)

We construct a hexagonal lattice of repressing genes, such that each node represses three of the neighbors, and use it as a model for genetic regulation in spatially extended systems. Using symmetry arguments and stability analysis we argue that the repressor-lattice can be in a non-frustrated oscillating state with only three distinct phases. If the system size is not commensurate with three, oscillating solutions of several different phases are possible. As the strength of the interactions between the nodes increases, the system undergoes many transitions, breaking several symmetries. Eventually dynamical frustrated states appear, where the temporal evolution is chaotic, even though there are no built-in frustrations. Applications of the repressor-lattice to real biological systems are discussed.

PACS numbers: 05.45.-a,87.18.Hf

Our understanding of genetic regulation inside the cell has greatly improved in recent years. A number of genetic circuits have been quantitatively characterized, ranging from switches to oscillators made up of negative feedback loops. The latter class of circuits is ubiquitous in regulatory networks with oscillating gene expressions, two of the most important examples being the NF κ B network for inflammatory response [1, 2, 3] and the p53-mdm2 system which regulates cell apoptosis [4, 5].

However, decisions taken inside the cell may depend crucially on the environment and may be cooperative, i.e. depend on the behavior of neighboring cells. This calls for theoretical modeling which explicitly takes the spatial arrangement of different cells into account. As a basic unit, we consider a negative feedback loop consisting of three proteins that repress each other by blocking the associated genes, which Leibler and Elowitz termed the 'repressilator' [6]. Previously, others have studied coupled repressilators to investigate quorum sensing [7] and cell-to-cell communication [8]. As a further step, one might consider systems made up of regular arrays of cells interacting in a specific manner with neighboring cells. Because of close packing, real arrays of cells in planar tissues often display hexagonal or near-hexagonal structure, e.g. in hepatic or retinal tissue [9, 10, 11].

Here we approach this general problem by extending the simple repressilator to a repressor-lattice – a hexagonal array of repeated and overlapping repressilator motifs, as shown in Fig. 1. Each node is repressed by three neighboring nodes and at the same time represses three other neighbors. A biological implementation of such a system would require a tissue where cells communicate specifically with their immediate neighbours, rather than in a mean-field manner as in quorum sensing. Such direct communication is in fact quite common, either through small conduits that connect the cells, or via proteins that span the membrane of the cells [12]. Further, the directed nature of the interactions would require some

form of epigenetic gene silencing, resulting in adjacent cells expressing different genes even though they have exactly the same DNA [13, 14, 15]. The modeling framework we propose is, however, general and can be used to describe other kind of interactions, such as bidirectional ones, which might be easier to realize experimentally.

The lattice in Fig. 1 can be naturally constructed to be translationally invariant and such that all local loops are repressilator motifs. We will approach the problem by imposing periodic boundary conditions in order to preserve translational invariance. Later, we will discuss how these results translate to the case of a large lattice without the periodic boundary conditions, which is more relevant for biology.

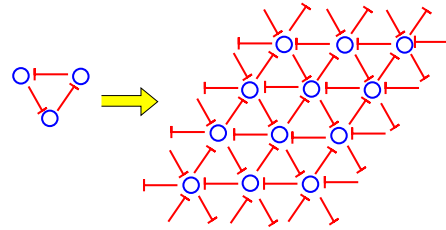


FIG. 1: The construction of the repressor-lattice from 'units' of single repressilators suitably placed on a hexagonal lattice. Each link symbolizes a repressor between two nodes corresponding to repressing genes, proteins, species, etc.

The basic repressilator motif may exhibit an oscillating state with a phase difference between consecutive variables equal to $2\pi/3$. One can ask whether the entire repressor-lattice might exist in an oscillatory state where only three different phases are allowed, each differing by $2\pi/3$. We will show that this is indeed the case, but lattice commensurability effects may break this scenario.

In the repressor-lattice, the variable at a node (m, n) is repressed by three neighboring nodes which we represented by an interaction term F_{int} , leading to a dynamical

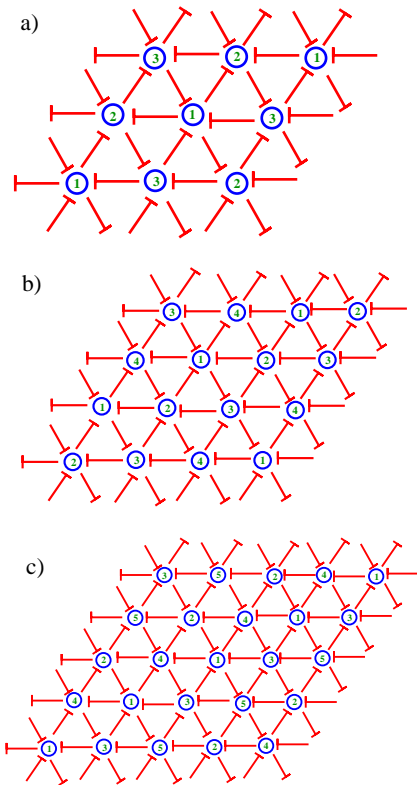


FIG. 2: Systems of 3×3 (a), 4×4 (b) and 5×5 (c) nodes subjected to periodic boundary conditions as indicated by the extra links. The numbers refer to the different phases of the solutions just above Hopf bifurcations. In (a) the solution exhibits symmetry with respect to rotations of angles which are multiples of $2\pi/3$. In (b), (c) this symmetry is broken, so that 3 distinct solutions coexist above the Hopf bifurcation.

cal equation for the concentration of species $x_{m,n}$:

$$\frac{dx_{m,n}}{dt} = c - \gamma x_{m,n} + \alpha F_{int} \quad (1)$$

We consider two types of interaction terms – either an additive repression (an ‘or gate’):

$$F_{int} = \frac{1}{1 + \left(\frac{x_{m+1,n}}{K}\right)^h} + \frac{1}{1 + \left(\frac{x_{m,n-1}}{K}\right)^h} + \frac{1}{1 + \left(\frac{x_{m-1,n+1}}{K}\right)^h} \quad (2)$$

or a multiplicative repression (an ‘and gate’):

$$F_{int} = \frac{1}{1 + \left(\frac{x_{m+1,y}}{K}\right)^h} \cdot \frac{1}{1 + \left(\frac{x_{m,n-1}}{K}\right)^h} \cdot \frac{1}{1 + \left(\frac{x_{m-1,n+1}}{K}\right)^h} \quad (3)$$

In either case we use standard Michaelis-Menten terms to model the repression. The parameter c measures the constitutive production of the proteins, γ determines the degradation rate and α the strength of the repression by another protein. Further, K is the dissociation constant of the binding complex whereas h is the Hill coefficient measuring its cooperativity. For simplicity we assign the same parameter values to all the nodes in the lattice. We

note that Ref. [6] also introduced the associated mRNA for each gene resulting in six coupled ordinary differential equations. For simplicity we keep only the protein variables leading to three coupled equations – a single repressor with this simplification can still be brought into an oscillating state [16].

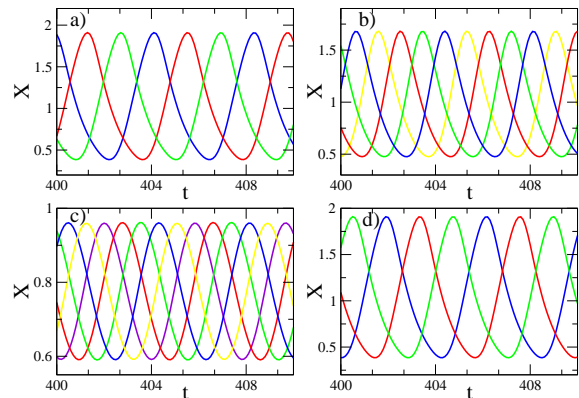


FIG. 3: Solutions of repressor-lattices of sizes a): 3×3 , b): 4×4 , c): 5×5 , d): 6×6 with multiplicative interactions, Eq. (3) and parameters $c = 0.1, \gamma = 1.0, K = 1.0, h = 2$. The value of α is in each case chosen to be just above the Hopf bifurcation. Note that three, four and five different phases exist in a), b), c), respectively. In d) there are however only three different phases.

For a single repressor there exists a large regime of parameter space where oscillations are possible [6, 16]. The transition to oscillations occurs via a Hopf bifurcation. We find similar behavior in the repressor-lattice. As a starting point, a lattice with 3×3 nodes as in Fig. 2a was simulated both with additive, Eq. (2), and multiplicative, Eq. (3), couplings. Just above the Hopf bifurcations, we found smooth oscillations with only three distinct phases as indicated by the numbers 1,2,3 labeling the nodes in Fig. 2a. The oscillating time series is shown in Fig. 3a. These solutions are trivially related to the solutions of the basic repressor motif since each node receives three identical inputs, with a $2\pi/3$ phase shift with respect to itself. Note that this solution is invariant under lattice rotation of multiples of $2\pi/3$

However, this scenario is not completely general. For instance, in the case of a lattice of size 4×4 (16 nodes) the corresponding dynamical solutions are different, as shown in Fig. 3b. As in the previous case (Fig. 3a) we are relatively close to the first Hopf bifurcation. However, now phases of the oscillating solutions differ by $2\pi/4$ between the nodes. The origin of this is a commensurability effect between the number of nodes in the lattice and the associated number of possible phases of the oscillating solutions. This commensurability effect is of course enforced by the periodic boundary conditions. The complete structure of the phases is shown on the 4×4 unit cell in Fig. 2b. The case of 5×5 is also affected by

commensurability effects, as shown in Figs. 2c and 3c.

As opposed to the 3×3 system, here the inputs arriving to a specific node are different. This reflects the fact that the oscillatory solution is no longer rotationally invariant. We note that all lattices which are commensurate by three, i.e. 6×6 (see Fig. 3d), 9×9 , etc, allow a non-frustrated, symmetric state similar to the 3×3 system. These periodic solutions all exhibit a Goldstone mode in the sense that it is possible to slide the phases as long as the phase differences are kept constant. This means that the specific values of the phases for the solutions are determined by the initial conditions.

In order to understand these solutions in depth, we perform a stability analysis. We consider the ‘‘or’’ gate Eqs. 1,2 and, since the system is translationally invariant, we search for a constant homogeneous solution:

$$x_{m,n} = x^* \quad \forall m, n \quad \longrightarrow \quad 3\alpha K^h = (\gamma x^* - c)(K^h + x^{*h}). \quad (4)$$

The equation for x^* always has one, and only one, real positive solution. The next step is to perturb the homogeneous solution in order to perform a stability analysis. We consider a first order perturbation of the form:

$$x_{m,n}(t) = x^* + \epsilon \exp \left[\lambda t + \frac{2\pi i(k_m m + k_n n)}{L} \right]. \quad (5)$$

Notice that since the solution must have the periodicity of the lattice, k_m and k_n should be natural numbers and also $1 \leq k_m, k_n \leq L$. Plugging the solution into Eq. (1) and expanding to first order in ϵ yields the following dispersion relation:

$$\lambda = -\tilde{a} \left(e^{\frac{2\pi i k_m}{L}} + e^{-\frac{2\pi i k_n}{L}} + e^{\frac{2\pi i(k_n - k_m)}{L}} \right) - \gamma, \quad (6)$$

where $\tilde{a} = \alpha h K^h (x^*)^{h-1} / [K^h + (x^*)^h]^2$. Other kind of interaction terms lead to the same dispersion relation simply with a slightly different definition of x^* and \tilde{a} ; for example, taking multiplicative interactions leads to $\tilde{a} = \alpha (h/K) (x^*/K)^{h-1} / [1 + (x^*/K)^h]^4$. Eigenvalues λ with a positive real part will destabilize the homogeneous solution. Taking the real part of expression (6), the eigenvalue with the largest real part is the one that minimizes the function:

$$f(k_m, k_n) = \cos \left(\frac{2\pi k_n}{L} \right) + \cos \left(-\frac{2\pi k_m}{L} \right) + \cos \left(\frac{2\pi(k_m - k_n)}{L} \right). \quad (7)$$

Before finding the solutions, we stress that $f(k_m, k_n) = f(-k_m, -k_n)$, while the imaginary part of the eigenvalue changes sign when the wave vector changes sign. This means that the two vectors (k_m, k_n) and $(-k_m, -k_n)$ minimizing the function f are the complex conjugate pair that will cause the Hopf bifurcation. The function f is independent of the parameters of the system, meaning that the kind of pattern depends not on the form of the

interaction (as long as the lattice is homogeneous with the same geometry), but on the number of sites in the lattice. The value of γ determines only how much we have to increase \tilde{a} to encounter the Hopf bifurcation.

Plotting the function $f(k_m/L, k_n/L)$ in the first Brillouin zone, $0 \leq k_m, k_n < L$ we see that it achieves its absolute minimum for the couple of eigenvalues $(k_m/L, k_n/L) = (1/3, 2/3)$ and $(k_m/L, k_n/L) = (2/3, 1/3)$, where $f(k_m, k_n) = -3/2$, see Fig. 4. This means that a Hopf bifurcation will occur when $3\tilde{a} = 2\gamma$. Of course these wave vectors are allowed only when L is a multiple of 3, so that the values of k_m and k_n at the minimum are natural numbers.

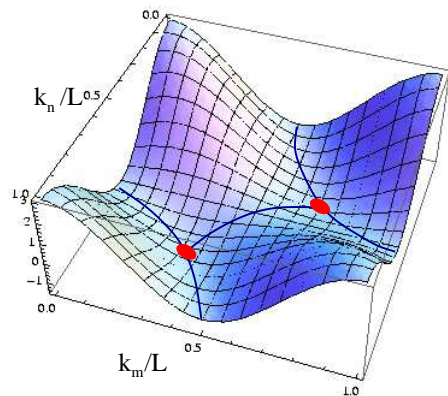


FIG. 4: The landscape of the function Eq. (7). Red dots mark absolute minima, corresponding to the symmetric solution for L multiple of 3. Blue lines mark the bottom of the valleys around the minima. When L is not multiple of 3, the absolute minima are not achievable, and the degenerate solutions are given by 3 complex conjugate pairs along these valleys.

We can of course minimize the function f also for values of L that are not multiples of 3. For $L = 4$, the minimum is $f(1, 3) = f(3, 1) = -1$, but also $f(2, 3) = f(3, 2) = -1$ and $f(3, 4) = f(4, 3) = -1$. The case $L = 5$ is also a degenerate case. The minimum is $f(2, 3) = f(3, 2) \approx -1.30902$, but also $f(1, 3) = f(4, 2) \approx -1.30902$ and $f(2, 4) = f(3, 1) \approx -1.30902$. All cases that are not multiples of 3 have this degeneracy, due to the symmetry of the lattice. Close to the Hopf bifurcation, the number of observed phases will reflect the periodicity of the eigenfunction. In particular, there will always be 3 distinct phases if L is a multiple of 3 and L phases if L is a prime number.

The phases of the eigenfunctions can be used to figure out how the oscillation pattern will look like on the lattice: sites on the lattice at a distance $\Delta m, \Delta n$ such that $k_m \Delta m + k_n \Delta n = 0$ will be in phase. Fig. 2c shows one of these solutions of the 5×5 lattice, namely $f(4, 1)$. The other ‘symmetric’ solutions can be obtained through rotations of multiples of $2\pi/3$, respecting the hexagonal rotational symmetry of the lattice.

One might expect that the symmetric solutions with

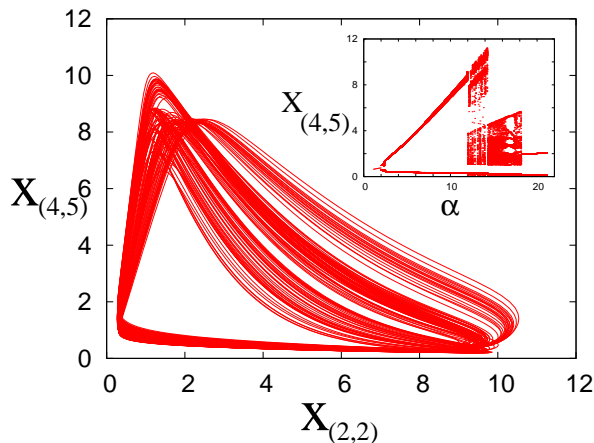


FIG. 5: A specific chaotic solution for a 5×5 lattice with multiplicative coupling (Lyapunov exponent equal to 0.028) obtained at a coupling strength equal to $\alpha = 12.8$ with the variable in node $(4, 5)$ plotted against the variable in node $(2, 2)$. Other parameter values are: $c = 0.1, \gamma = 1.0, K = 1.0, h = 3$. Inset: Bifurcation diagram, showing the maxima and minima for dynamical solutions in the node point $(4, 5)$ after a transient period of 15000 time units. The extremal values are plotted against varying values of the coupling strength α . The critical value for the Hopf bifurcation calculated from the dispersion relation 6 (see main text) gives $\alpha_c = 1.838$.

five different phases, Fig. 2c, could exist even when parameters are varied. This is not the case: when the coupling parameter α is increased, several transitions related to strong non-linear effects take place. Starting out with smooth periodic solutions of five distinct phases, amplitude modulations set in when the coupling constant $\alpha \approx 2.6$. At the same parameter value, we also observe that some phases that were distinct before this transition now coalesce with each other. At higher α -values, amplitude modulations become even more pronounced and furthermore temporal period-doubling sets in. Increasing α even more, chaotic solutions eventually appear as shown in the bifurcation diagram and the attractor of Fig. 5 (similar bifurcation diagrams are observed for repressive cell-cell communication [8]). Even though the lattice is made up of simple repressilators without local frustration, the resulting dynamics is chaotic: it is not possible to keep the simple five-phase solutions when the repressilators are coupled strongly with the neighbors. Each node in the 5×5 lattice exhibits a different bifurcation diagram (no simple period five symmetry operations are present) showing that all symmetries are eventually broken through a series of non-linear transitions.

One may wonder how realistic periodic boundary conditions are for modeling real biological systems. In the 3×3 case, this might be implemented in a single cell with 9 different genes, each repressed by three different ones. Having in mind extended systems, a more realistic case is to consider a large, finite lattice with non-periodic

boundary conditions to represent an isolated planar tissue, in which cells at the boundary receive no external signal. We found from simulations that such a system shows frustration effects similar to the case of periodic boundaries: when the steady state is destabilized, cells far from the boundaries exhibit the three-phase dynamics of the repressilator circuit, while closer to the boundaries the dynamics is more irregular, with more phases possible. We did not observe any chaos in this case, even for very large values of α .

In conclusion, the lattice model we have investigated here provides a simple starting point to study regulation in spatially extended biological systems. Future direction could include, for instance, introducing an intrinsic 'frustration' in the repressor-lattice. There are several ways of doing this, e.g. by lattice defects, or mutations modifying some of the interactions. For example, one can consider what happens when a specific repressor link is mutated into an activator. These generalizations may provide a useful framework for describing more specific cases of cell-to-cell communication in biological tissues.

We are grateful to Namiko Mitarai, Joachim Mathiesen and Szabolcs Semsey for discussions. This work is supported by Danish National Research Foundation.

* Electronic address: mhjensen@nbi.dk

† URL: <http://cmol.nbi.dk>

- [1] D.E. Nelson, A.E.C. Ihekweaba, M. Elliott, J.R. Johnson, C.A. Gibney, B.E. Foreman, G. Nelson, V. See, C.A. Horton, D.G. Spiller *et al. Science* **306**, 704 (2004).
- [2] A. Hoffmann, A. Levchenko, M.L. Scott and D. Baltimore, *Science* **298** 1241–1245 (2002).
- [3] S. Krishna, M.H. Jensen and K. Sneppen, *Proc. Natl. Acad. Sci. USA* **103**, 10840–10845 (2006).
- [4] N. Geva-Zatorsky, N. Rosenfeld, S. Itzkovitz, R. Milo, A. Sigal, E. Dekel, T. Yarnitsky, P. Pollack, Y. Liron, Z. Kam, G. Lahav and U. Alon, *Mol. Sys. Biol.* **2**, E1-E13 (2006).
- [5] G. Tian, S. Krishna, S. Pigolotti, M.H. Jensen, and K. Sneppen, *Phys. Biol.* **4**, R1–R17 (2007).
- [6] M.B. Elowitz and S. Leibler, *Nature*. **403**, 335-8 (2000).
- [7] J. Garcia-Ojalvo, M.B. Elowitz and S.H. Strogatz, *Proc. Natl. Acad. Sci.* **101**, 10955-10960 (2004).
- [8] E. Ullner, A. Zaikin, E.I. Volkov, and J. Garcia-Ojalvo, *Phys. Rev. Lett.* **99**, 148103 (2007); E. Ullner, A. Koseska, J. Kurths, E.I. Volkov, H. Kantz, and J. Garcia-Ojalvo, *Phys. Rev. E* **78**, 031904 (2008).
- [9] J.P. Revel and M.J. Karnovsky, *Jour. Cell Biol.* **33** C7 (1967).
- [10] H Sawada, H Konomi and K Hirosawa, *Jour. Cell Biol.* **110**, 219-227 (1990)
- [11] G. Vozzi, A Previti, D. De Rossi, A. Ahluwalia, *Tissue Engineering* **8**, 1089–1098 (2002).
- [12] S. F. Gilbert, *Developmental Biology*, 6th Edition, Sinauer Associates Inc., Sunderland, Massachusetts (2000).
- [13] A. P. Bird, A. P. Wolffe, *Cell* **99**, 451–454 (1999)
- [14] T. Suzuki, N. Miyata, *Curr. Med. Chem.* **13**, 935–958

- (2006).
- [15] I. B. Dodd, M. A. Micheelsen, K. Sneppen, G. Thon, *Cell* **129**, 813–822 (2007).
- [16] S. Pigolotti, S. Krishna, M. H. Jensen, *Proc. Natl. Acad. Sci.* **104**, pp. 6533–6537 (2007).